The Royal Society

The influence of magnetic field and pressure on the structural phase transition in $La_{1-x}Sr_xMnO_3$

By Don McK. Paul[1], K. V. Kamenev[1], A. J. Campbell[1], G. Balakrishnan[1], M. R. Lees[1] and G. J. McIntyre[2]

[1]*Department of Physics, University of Warwick, Coventry CV4 7AL, UK*
[2]*Institut Laue-Langevin, BP 156X, 38042, Grenoble Cedex 9, France*

Neutron diffraction techniques have been used to investigate the influence of applied magnetic field and pressure on the structural and magnetic phase transitions in $La_{1-x}Sr_xMnO_3$. The structural, magnetic and electronic properties are found to be strongly coupled. For suitable compositions the coupling between the magnetism and the crystal structure becomes so strong that the structural phase transition may be driven by the application of a magnetic field. The influence of pressure on both the structural and ferromagnetic phase transition is summarized in a pressure–temperature phase diagram. This diagram reveals several unusual features, including the pressure independence of the Curie point in the orthorhombic phase, a re-entrance of the rhombohedral phase at low temperatures, and a change of order of the magnetic phase transition.

Keywords: neutron diffraction; structural phase transition; magnetic phase transition; field induced transition; pressure dependence; manganites

1. Introduction

The discovery of colossal magnetoresistance (CMR) in distorted manganese perovskites of type $(R_{1-x}A_x)MnO_3$, where R is a rare earth ion and A represents a divalent alkaline earth ion, has led to a renewed interest in the general physical properties of these materials. Considerable effort has been concentrated on measuring the structural, magnetic and electronic properties of such compounds with the aim of gaining a better understanding of the microscopic origins of CMR and other aspects of the influence of the strong coupling between magnetism, crystal and electronic structure.

The manganites exhibit a rich variety of magnetic and structural phase transitions. The pioneering work of Wollan & Koehler (1955) who examined the structural forms and magnetic ordering in $La_{1-x}Ca_xMnO_3$ as a function of doping and temperature, clearly demonstrated the power of neutron diffraction in identifying the various states. A similar extensive investigation of $Pr_{1-x}A_xMnO_3$, where A = Ca, Sr or Ba, was described in a series of papers by Jirak *et al.* (1985) and Knizek *et al.* (1992) and again illustrates the importance of neutron measurements for these systems. The advantage of using neutrons for such diffraction studies is primarily because the neutron carries a magnetic moment and is therefore sensitive to the magnetic correlations in the material. In addition, the neutron is sensitive to the arrangement of the oxygen atoms around the Mn site allowing an accurate picture of the structural rearrangement to be extracted from neutron experiments. More recent

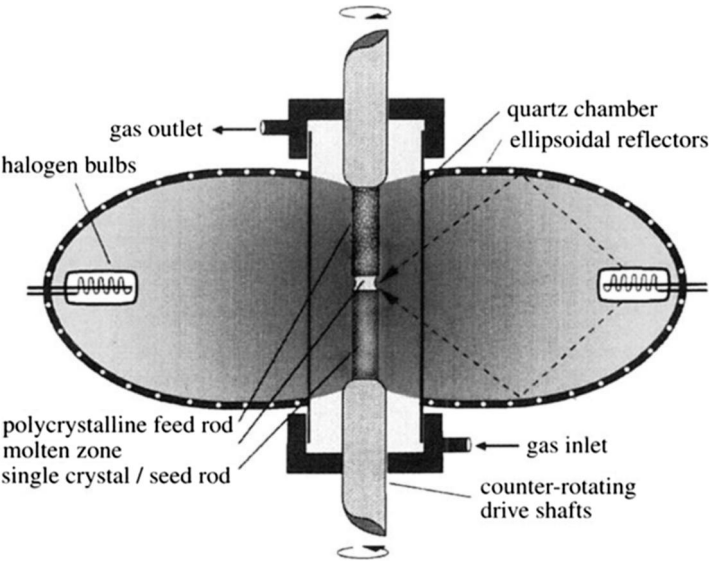

Figure 1. An annotated sketch of an infrared image furnace which has been used to grow single crystal samples of $La_{1-x}Sr_xMnO_3$. The various parts of this instrument are described in the text.

work making use of higher flux and resolution has added to this body of knowledge and emphasised the complexity and subtlety of the interaction between structure, magnetism and electronic effects (see, for example, Radaelli *et al.* 1996).

This paper will focus on the structural transformations in $La_{1-x}Sr_xMnO_3$ and discuss how the change in structure is influenced by doping, and in more detail how the application of a magnetic field or the application of pressure can alter the phase diagram at a particular doping. All the work in this paper has been performed with single crystal samples and we therefore begin with a description of the method used to produce high quality, single crystal samples of these materials. This section is followed by a brief description of the structural and magnetic phase diagram as a function of doping, followed by direct, microscopic evidence for the forcing of a structural rearrangement by the application of an applied magnetic field and the unusual phase diagram for a doped manganite under pressure. Finally, we attempt to draw these various strands together to comment on the coupling between magnetism and structural rearrangement in this material.

2. Crystal growth of the manganites

In this work, and in many other studies of the physical properties of the manganites, it is essential to have available large, single crystal samples of these materials. Fortunately, it is possible to grow such crystals using a 'floating zone' technique in an infrared image furnace (see figure 1). A brief description of this method of crystal growth and the conditions we have found appropriate for such growths are given below.

The floating zone method which has been successfully used in the past to produce large and high quality crystals of many oxides, is also applicable to the growth of

the manganites. This method overcomes most of the drawbacks encountered in the more commonly used 'flux growth' techniques, such as flux inclusion in crystals and contamination from the crucible material. The method involves the use of an infrared image furnace which is schematically illustrated in figure 1. This furnace operates by focusing light from two halogen lamps placed at the focal points of the two semi-ellipsoidal chambers, on to the sample position, which is at the joint focal point of the two chambers. The sample melting is controlled by the power supplied to the lamps, and during growth the crystal can be viewed through a camera, allowing adjustment of the growing conditions in response to changes seen in the molten zone. The sample area is enclosed in a quartz tube and various pressurized, gaseous atmospheres may be used to control evaporation and maintain stoichiometry in the grown material. Crystal growth is initialized by forming a molten zone between a feed (sample of appropriate composition) and a seed (crystal or polycrystalline) rod. These two rods are counterrotated to achieve the homogenization of composition and temperature within a stable molten zone. The crystal is grown by synchronously scanning the molten zone along the feed rod. It is also possible to use a seed rod which is rich in a flux for the material and to essentially perform a scanned flux method.

The family of compounds $R_{1-x}Sr_xMnO_3$ lends itself readily to crystal growth by the 'floating zone' method. Crystals of $La_{1-x}Sr_xMnO_3$ and $Pr_{1-x}Sr_xMnO_3$, for neutron scattering measurements, have been grown using the infrared image furnace. Polycrystalline materials were first synthesized starting from high purity La_2O_3, Pr_6O_{11}, $SrCO_3$ and MnO_2. Stoichiometric amounts of the powders were ground together and calcined at 1300 °C and 1350 °C for 12 h each with intermediate grindings. The material was then isostatically pressed into rods (typically 6–8 mm diameter and 80 mm long) and sintered at 1350 °C for 12 h. The crystal growth was carried out using a double ellipsoidal infrared image furnace, in air. The growth rate was 6–8 mm hr^{-1} and the two rods were counterrotated at 20–30 RPM. The crystals were examined for quality by X-ray Laue techniques and basic characterization measurements were carried out in our laboratory to determine the temperatures of the structural and magnetic phase transitions.

Individual crystals for resistivity, AC susceptibility, magnetization, pressure and neutron diffraction experiments were cut from the grown boule. The as-grown boule, or a portion of it, was also used for neutron inelastic scattering experiments.

3. Phase transitions as a function of composition

$La_{1-x}Sr_xMnO_3$, can adopt two structural variants depending on the doping and a range of other conditions, when prepared under ambient oxygen pressure (a more distorted form with $P2_1/c$ structure also exists if the material is prepared under an atmosphere which is low in oxygen (Mitchell *et al.* 1996)). The structural transition in $La_{1-x}Sr_xMnO_3$ is from a high temperature rhombohedral phase ($R\bar{3}c$) to a low temperature orthorhombic phase ($Pbnm$). Figure 2 illustrates these two possible structures by presenting in (a) and (c) the rhombohedral unit cell, in a hexagonal setting, and the orthorhombic variant. Only the MnO_6 octahedra are displayed in these figures. In figure 2b, d a set of eight octahedra are shown which would have formed a cubic unit cell, if there was no distortion resulting in the formation of a structure with a lower symmetry. In the rhombohedral phase the Mn atom is located at the centre of a nearly regular octahedron with all the Mn–O bond distances having

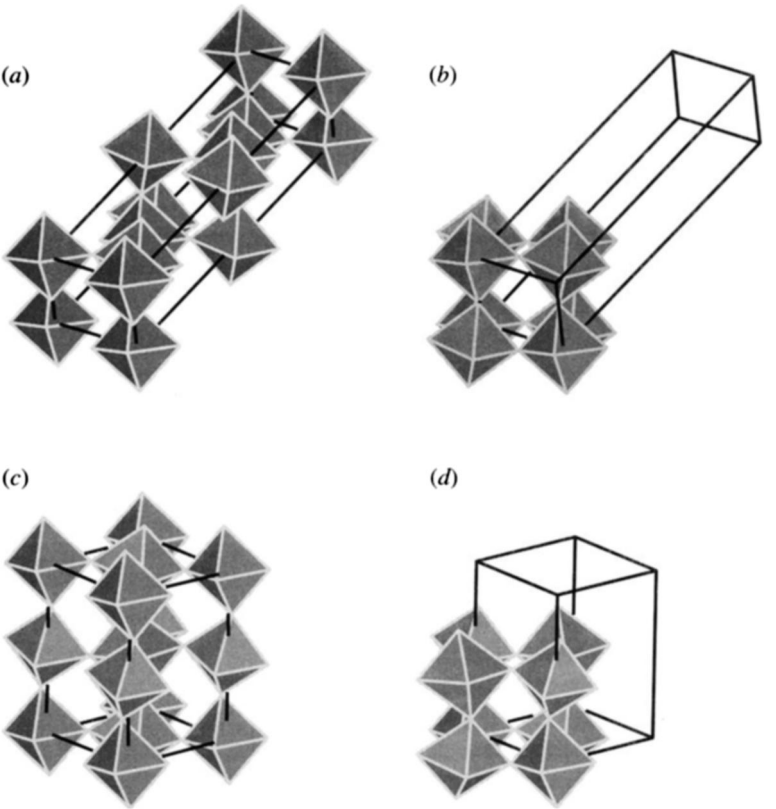

Figure 2. Various views of the rhombohedral and orthorhombic structures which can be adopted by $La_{1-x}Sr_xMnO_3$. Only the MnO_6 octahedra are shown in this figure. The scale of this figure is appropriate for $La_{0.835}Sr_{0.165}MnO_3$ just above and below the structural phase transition in zero field and zero applied pressure. (*a*) The unit cell in the rhombohedral phase. (*b*) Eight octahedra which would form a cubic cell if no rhombohedral distortion were present. (*c*) The unit cell in the orthorhombic phase. (*d*) Eight octahedra which would form a cubic cell if no orthorhombic distortion were present.

the same length. The La(Sr) are randomly distributed over equivalent 12-fold coordinated sites at the centre of a set of eight octahedra. A three-dimensional network of octahedra is formed by joining the vertices of the octahedra. The octahedra in the rhombohedral phase are tilted along what would have been a [1 1 0] direction in a cubic form of this material. In the orthorhombic phase the octahedra are irregular. The distorted octahedra have three different Mn–O bond distances, one between the Mn and the axial oxygen and two between Mn and the oxygens in the equatorial plane. There are also two tilt angles for the octahedra in this structure, one between octahedra in what was the cubic *a*–*b* plane (this angle being very similar to the tilt in the rhombohedral structure) and a tilt between octahedra along the cubic *c*-axis. The magnitudes of these tilt angles and bond lengths are very important quantities in determining the degree of electronic hopping which can occur and hence may have a drastic influence on the transport properties of the material. The phase transition from a rhombohedral to an orthorhombic structure is considered to be a cooperative

Jahn–Teller distortion produced as a consequence of the orbitally degenerate electronic state of the Mn^{3+} ion in an octahedral crystal field. As temperature is lowered, at a constant Sr (or equivalently Mn^{4+}) doping, the energy gained by removing the electronic degeneracy will become greater than the energy penalty from distorting the network of octahedra, and a cooperative distortion of the octahedral network will take place at some temperature. Since it is not possible to continuously shift from one arrangement of octhedra to the other (*Pbnm* is not a symmetry subgroup of $R\bar{3}c$), this phase transition will be of first order.

The temperature, T_s, at which the structural transition occurs is strongly dependent on the level of Sr doping, x (Tokura *et al.* 1994; Kawano *et al.* 1996). For example, as x increases from 0.15 to 0.175, T_s decreases from 380 to 190 K. Undoped ($x = 0.0$) $LaMnO_3$ is an antiferromagnetic insulator; however, for doping levels $x > 0.1$ the compound has a ferromagnetic ground state. This ferromagnetic ground state can be qualitatively explained in terms of the double exchange interaction (first proposed by Zener (1951)) between Mn^{3+} and Mn^{4+} ions via intermediate O sites. However, Millis *et al.* (1995) have shown that double exchange alone cannot explain the magnitude of the magnetoresistance that is observed. The Curie temperature, T_C, is also influenced by the level of doping but in contrast to T_s, T_C increases from 238 to 283 K as the doping is increased from 0.15 to 0.175. Figure 3 shows T_C and T_s as a function of the x in the vicinity of these doping values. It should be noted that the transition temperatures for our single crystals are systematically shifted from the values quoted in the work of Asamitsu *et al.* (1995). The values and properties of our $x = 0.165$ sample is identical to their sample with $x = 0.17$. The differences in T_C and T_s between the crystals grown by us, and those used in the work of Asamitsu *et al.* for the same nominal starting composition, are possibly due to the rapid variation of T_C and T_s with x and slight variations in oxygen stoichiometry which can affect these transition temperatures. This is discussed in some detail by Mitchell *et al.* (1996). However, from the x–T phase diagram, it is clear that if the doping can be controlled carefully then the temperatures of the two phase transitions may be forced to occur at the same temperature.

4. Phase transition in an applied magnetic field

In a study by Asamitsu *et al.* (1995) of $La_{0.83}Sr_{0.17}MnO_3$, including resistivity and striction measurements, it was inferred that in a limited range of doping the structural transition can be induced by application of a magnetic field.

In order to induce the structural transition in a magnetic field we required a sample in which the structural and magnetic phase transitions are close together with the ferromagnetic transition occurring below the structural transition. Based on the measurements of the transition temperatures shown in figure 3, single crystals with $x = 0.165$ and $x = 0.17$ were grown in the infrared image furnace at Warwick using the floating zone method. X-ray Laue photographs showed that the resulting samples were high quality single crystals. The crystals were then characterized in our laboratory by measuring the resistivity, AC susceptiblity, and magnetization as a function of temperature. Figure 4 shows the temperature dependence of the resistivity and magnetization (and inset AC susceptibility) for the single crystal with $x = 0.165$. The resistivity shows an increase at 296 K associated with the structural transition and a large decrease near the Curie point at around 264 K. The

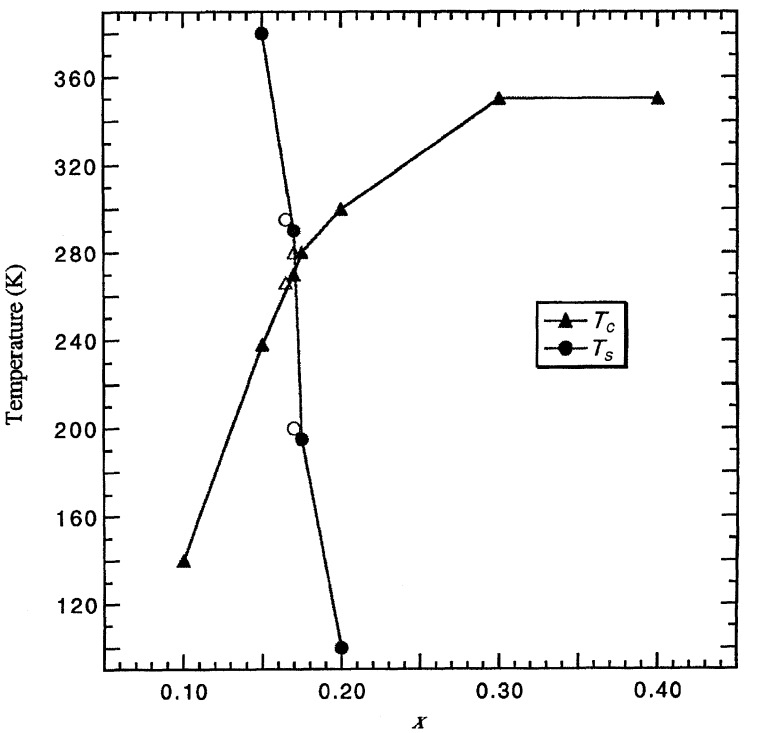

Figure 3. The temperatures of the structural transition, T_S, and the ferromagnetic transition, T_C, as a function of the doping x for single crystal $La_{1-x}Sr_xMnO_3$. Filled symbols are for the data of Tokura *et al.* and open symbols are data measured on our samples.

Curie point is sensitive to field and this is demonstrated by the magnetization and susceptibility data. The magnetization, measured in a field of 1 T, shows a T_C of 264 K; however, the AC susceptibility, measured in a field of 0.7 mT, showed a T_C of 261 K. There is hysteresis in the structural transition showing its first-order nature. Measurements on the $x = 0.17$ sample found a T_C of 283 K and a T_s of 183 K. From these measurements it was clear that our $x = 0.165$ sample satisfied the requirements for observing the proposed field induced structural transition, i.e. T_C and T_s close together with T_C below T_s.

Neutron-diffraction measurements were carried out at the reactor source of the Institut Laue-Langevin in Grenoble, France (Campbell *et al.* 1997). In a preliminary experiment on the single crystal diffractometer D10, extensive structural measurements were made, and by following the intensity of the (4 4 5) reflection, the temperature of the structural phase transition in zero applied magnetic field was confirmed to be 296 K. The (4 4 5) reflection is only present in the orthorhombic phase and so a measurement of its intensity gives a direct determination of the structural phase of the sample. The intensity of the (2 0 0) reflection was also measured as a function of temperature. The (2 0 0) is a weak nuclear reflection which shows a large increase in intensity at the onset of the ferromagnetic state. By measuring this reflection we were able to confirm the temperature of the magnetic transition as 261 K.

The field switching experiment was carried out on the polarized-neutron normal-beam diffractometer D3 which is equipped with a 4.6 T cryomagnet. In this experi-

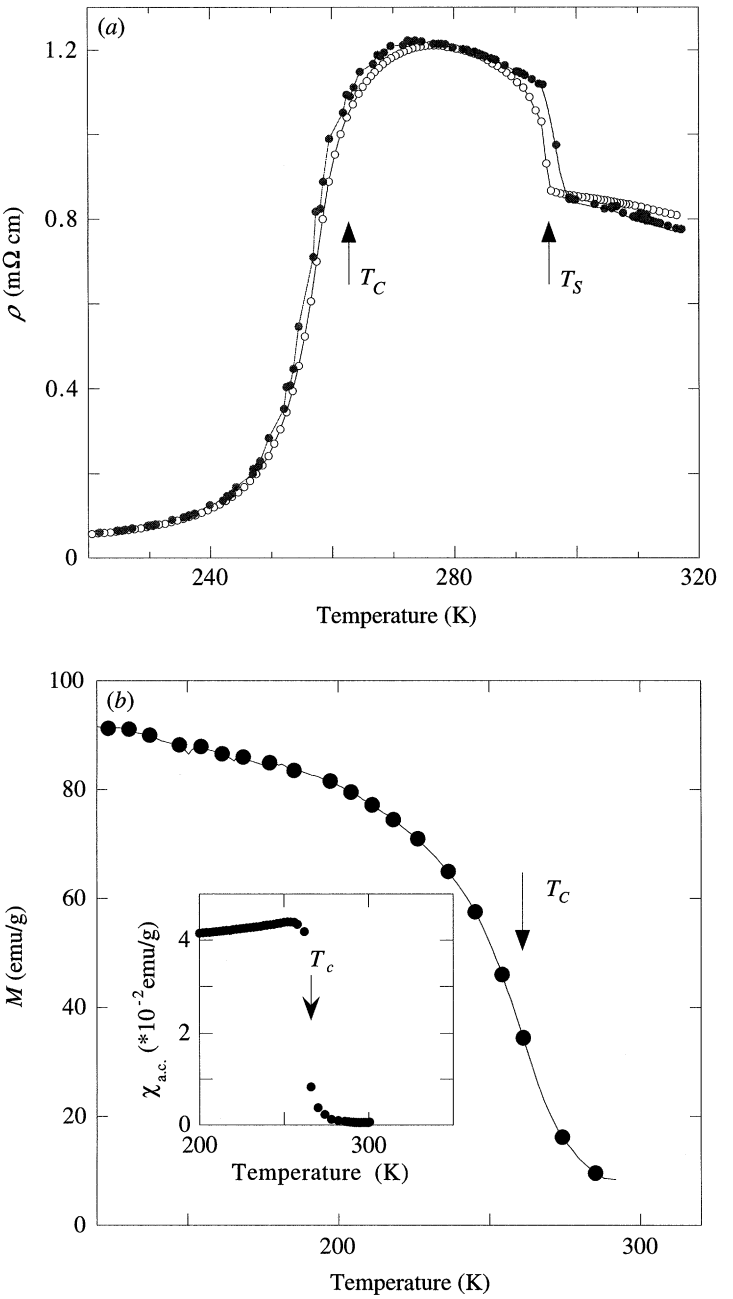

Figure 4. (*a*) Resistivity and (*b*) magnetization and inset AC susceptibility of single crystal $La_{0.835}Sr_{0.165}MnO_3$ as a function of temperature. The structural and magnetic phase transitions are marked with T_s and T_C respectively. (*a*) The resistivity was measured by a standard four-probe method, the open circles are for cooling and the filled circles are for warming. (*b*) The magnetization in a 1 T field was measured using a VSM and the AC susceptibility using a standard magnetic inductance technique with a frequency of 403 Hz and a field of 0.7 mT.

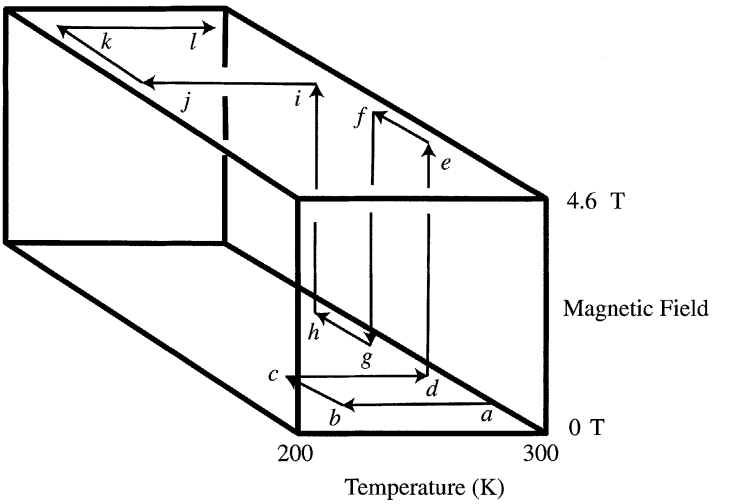

Figure 5. Schematic representation of the chronological sequence of temperature and magnetic field variations on the single crystal sample of $La_{0.835}Sr_{0.165}MnO_3$ during the experiment on D3 to observe the structural phase transition induced by a magnetic field.

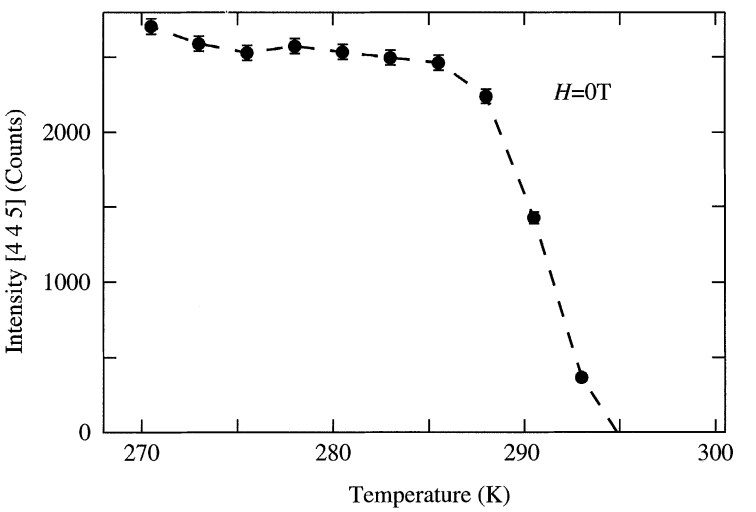

Figure 6. Intensity of a (4 4 5) reflection as a function of temperature (cooling) in zero magnetic field. The increase in intensity at 295 K shows the structural phase transition from the rhombohedral to the orthorhombic phase.

ment the intensities of the (4 4 5) and (2 0 0) reflections were measured as a function of temperature and magnetic field. The hysteresis in the system means that the chronological sequence of temperature and magnetic field changes during the experiment is important and this is shown schematically in figure 5. After the sample had been mounted and aligned it was cooled to 220 K (figure 5, $a \rightarrow b$). Figure 6 shows the intensity of the (4 4 5) reflection as a function of temperature. There is a clear increase in intensity starting at 295 K showing the structural phase transition

from the rhombohedral to the orthorhombic phase. At 220 K the transition to the orthorhombic phase was judged to be complete as the intensity of the (4 4 5) reflection had levelled out. The sample was then warmed to 290.5 K (figure 5, $c \rightarrow d$). At this temperature the sample is in the hysteretic region of the structural transition, but is still in the orthorhombic phase. It should also be noted that at 290.5 K the sample is in the paramagnetic phase.

At this temperature the magnetic field was gradually increased (figure 5, $d \rightarrow e$). Figure 7 shows the intensity of the (4 4 5) and (2 0 0) reflections as a function of magnetic field. In the first, increasing field, cycle the intensity of the (4 4 5) reflection shows a decrease in intensity beginning at about 2 T. By about 3 T the intensity has disappeared showing that the magnetic field has induced the structural transition from the orthorhombic phase to the rhombohedral phase. On decreasing the field (figure 5, $f \rightarrow g$) there is a slight increase in intensity below 2 T indicating that the sample partly transforms back into the orthorhombic phase, but is unable to transform back completely at this temperature. On increasing the field for a second time (figure 5, $h \rightarrow i$) the sample reverts to being fully rhombohedral.

The intensity of the (2 0 0) reflection presents an increase in intensity starting at about 0.5 T, showing that there is an increase in ferromagnetic alignment before the structural transition takes place. This indicates that the ferromagnetic alignment of the spins encourages the structural phase transition to the rhombohedral phase at this temperature. D3 has a polarized beam and so, by observing a flipping ratio, we were able to confirm the presence of a ferromagnetic contribution to the intensity of the (2 0 0) reflection. In a second measurement, we observed the structural phase transition as a function of temperature with the applied magnetic field fixed at 4.5 T and the resulting data are shown in figure 8. The temperature was decreased to 220 K (figure 5, $i \rightarrow j$) and at 270 K the crystal transforms into the orthorhombic phase. The fact that this transition occurs at 270 K in a field, compared to 296 K in zero field is again indicating that the ferromagnetic alignment of the spins favours the stability of the rhombohedral phase. The temperature was then increased to 290 K (figure 5, $k \rightarrow l$). The presence of hysteresis in such a constant field scan reflects the first-order nature of the transition, the hysteretic region is larger in an applied field than in zero field.

By using neutron scattering we have been able to directly observe and confirm the bulk nature of the magnetic field induced phase transition in $La_{0.835}Sr_{0.165}MnO_3$. At the temperature at which the experiment was performed removal of the field does not produce a switch back of structure and the transition is permanent, at least on the time-scale of these experiments.

5. Phase transition under pressure

The use of pressure as a thermodynamic variable provides us with a simple but powerful means by which to modify the interactions within the system at constant doping. The changes on a microscopic level influence transport and magnetoelastic properties and can be observed directly in the bulk properties. Measurements of the electrical resistivity and thermal expansion on a single crystal of $La_{0.835}Sr_{0.165}MnO_3$ were performed in a CuBe pressure cell with a fixed hydrostatic pressure of up to 9 kbar. The electrical resistivity was measured by standard four-point technique with the contacts glued onto a bar-shaped sample using silver-based epoxy. Micro-strain

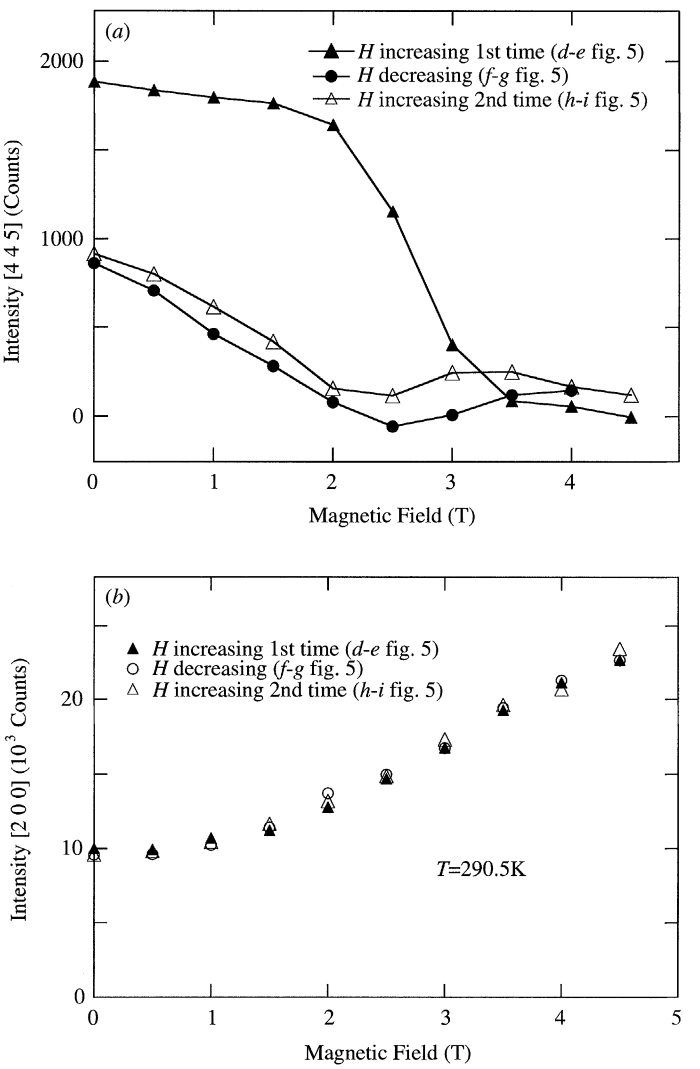

Figure 7. Intensity of the (*a*) (4 4 5) and (*b*) (2 0 0) orthorhombic reflections as a function of magnetic field at 290.5 K. (*a*) When the field is increased for the first time, the intensity of the (4 4 5) reflection disappears at *ca.* 3 T showing the transition to the rhombohedral phase. On decreasing the field, the intensity of the (4 4 5) reflection increases only slightly indicating a partial transformation to the orthorhombic phase. On increasing the field for the second time the intensity follows the same path as the decreasing field and the sample goes fully into the rhombohedral phase at high fields. (*b*) The intensity of the [2 0 0] reflection increases starting from *ca.* 0.5 T showing that there is an increased ferromagnetic alignment along the field direction.

gauges (Micro-Measurements Inc., SK-350) glued onto a bar-shaped crystal were used for the measurements of the thermal expansion. The strain gauges were calibrated using data for the thermal expansion and compressibility of silica, Cu, and Fe as references.

The temperature dependencies of electrical resistivity and thermal expansion mea-

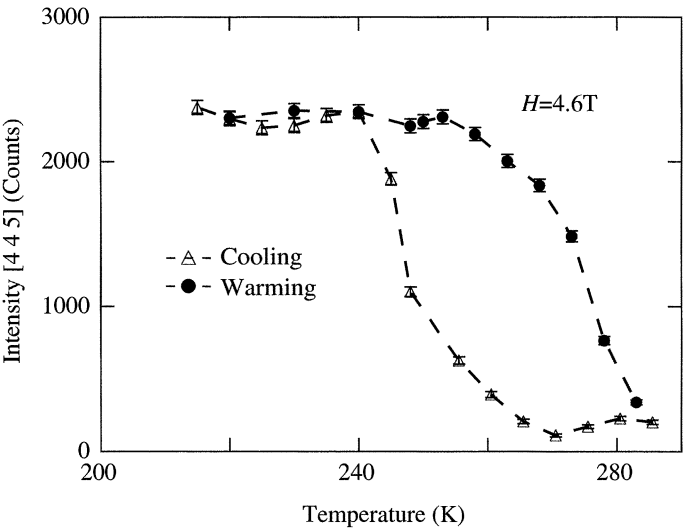

Figure 8. Intensity of the orthorhombic (4 4 5) reflection as a function of temperature in an applied magnetic field of 4.6 T field, demonstrating that there is a large hysteresis when the structural phase transition takes place under an applied field.

sured under 0, 5 and 9 kbar of starting pressure are presented in figure 9*a*, *b*, respectively. Because of differences in the thermal expansion coefficients of the pressure transmitting medium and the pressure cell, the pressure inside the cell decreased as the temperature lowered. The actual values of pressure at T_C and T_s for cooling and heating runs are shown in brackets. At ambient pressure, the sample undergoes a first-order phase transition from a high-temperature rhombohedral to a low-temperature orthorhombic state at $T_s = 295$ K; this transition is observed as a sharp decrease in striction of about 12% (see figure 9*b*). A second-order phase transition from a paramagnetic to ferromagnetic state takes place at $T_C = 261$ K and is accompanied by a gradual decrease in electrical resistivity. As pressure increases, T_C increases while T_s rapidly decreases. The crossing point of the magnetic and structural phase transitions can be achieved at 270 K by applying a pressure of about 3 kbar (Kamenev *et al.* 1997). Thus, application of pressure allows us to access four distinct regions in the pressure–temperature phase diagram due to the existence of a crossing point. Each of these phases is a combination of different types of magnetic (paramagnetic or ferromagnetic) and structural (orthorhombic or rhombohedral) ordering.

The measurements in the oil-pressure cell, allowing only pseudo-isobaric scans in temperature to be performed, have shown that the pressure dependence of T_C and T_s is remarkably nonlinear in the vicinity of the crossing point. As pressure increases from 1 to 3 kbar the temperature T_s decreases from 290 to 220 K whereas T_C increases from 263 to 278 K. To study directly the changes in the magnetic and structural phases of a single crystal of $La_{0.835}Sr_{0.165}MnO_3$ we have performed a neutron diffraction experiment in a high-pressure (up to 5 kbar) cell using gaseous helium as the pressure-transmitting medium, which enabled us to follow any chosen path in the 'pressure–temperature' (P–T) phase space. The neutron diffraction measurements were carried out using the single-crystal diffractometer D10 at the Institut Laue-Langevin. The orthorhombic (2 0 0) and (4 0 5) reflections were chosen

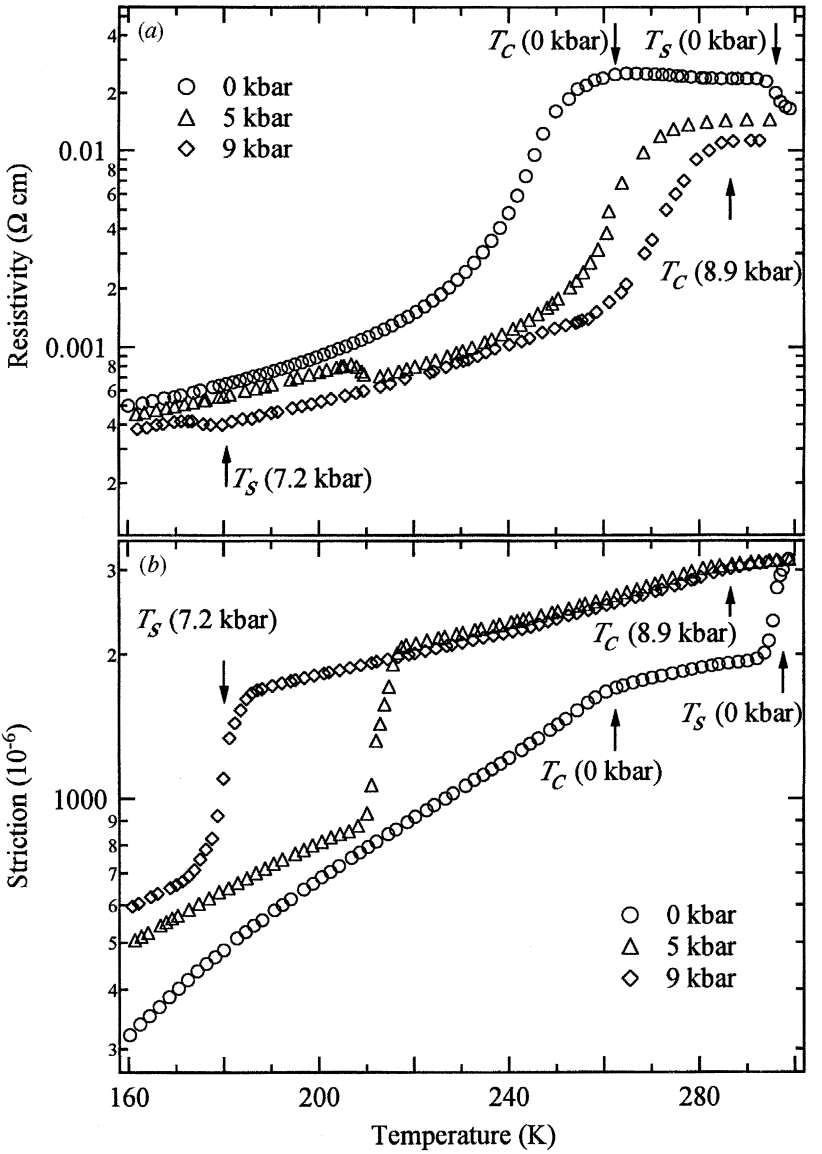

Figure 9. The temperature dependencies of (*a*) striction and (*b*) electrical resistivity for heating runs at starting pressures of 0, 5 and 9 kbar. The temperatures T_C and T_s are marked with arrows for the runs at 0 and 9 kbar. The actual pressures are shown in brackets.

to monitor the phase transitions, as they are clean indicators of the magnetic and structural state of the crystal respectively.

The P–T phase diagram of $La_{0.835}Sr_{0.165}MnO_3$ is shown in figure 10. The four possible phases are marked on the diagram as Pr, Po, Fo or Fr, where 'P' or 'F' specifies the magnetic state as paramagnetic or ferromagnetic while 'r' or 'o' describes the structural symmetry as rhombohedral ($R\bar{3}c$) or orthorhombic ($Pbnm$), respectively. The boundaries of the structural phase transitions are represented by the two

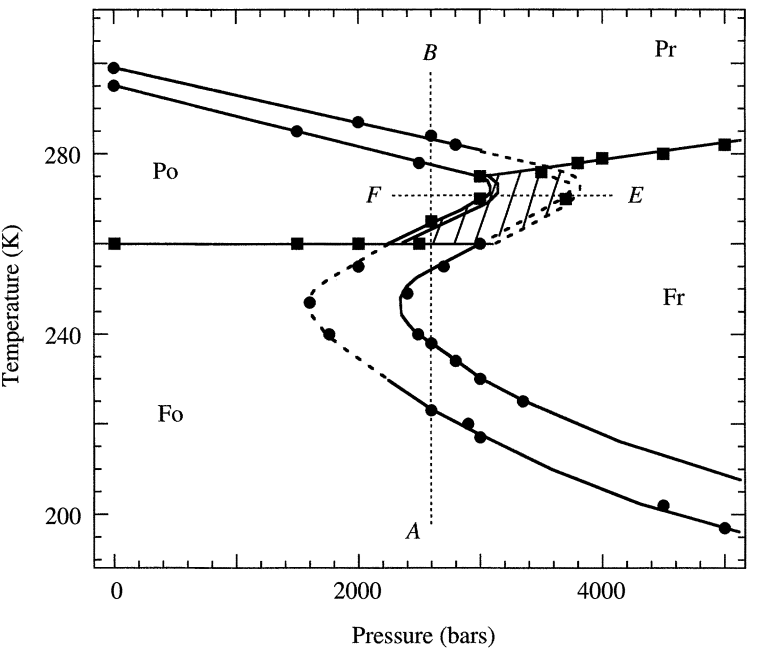

Figure 10. The structural and magnetic P–T phase diagram of $La_{0.835}Sr_{0.165}MnO_3$. The phases are Pr (paramagnetic: rhombohedral), Po (paramagnetic: orthorhombic), Fo (ferromagnetic: orthorhombic), Fr (ferromagnetic: rhombohedral). The Curie temperatures T_C and the temperatures of the structural phase transitions T_s are marked with square and circle symbols, respectively. The hatched area indicates the area of the crossing point.

'Z'-shaped curves indicating the metastability which is characteristic of a first-order phase transition. The magnetic phase transition is shown by the single line starting at $T_C = 261$ K, at ambient pressure, and ending at 282 K under a pressure of 5 kbar. The hatched area indicates the region of intersection of T_s and T_C and separates four phases, each with different combinations of structural and magnetic order. The portions of the phase boundaries which can be observed during a temperature scan at a constant pressure are delineated by solid lines. Due to the peculiar shape of the phase boundaries near the crossing point, some of the boundaries for the phase transitions cannot be detected by isobaric temperature scans alone. The phase boundaries which can be observed only in isothermal, pressure scans are shown by broken lines.

First we consider the phase diagram on the left and on the right of the hatched area. For less than 3 kbar, the temperature of the Pr → Po transition decreases linearly with applied pressure with a gradient of -6.1 K kbar^{-1} while the second-order Po → Fo magnetic phase transition seen at $T_C = 261$ K is pressure-independent. In sharp contrast, the Curie temperature in the rhombohedral phase increases linearly with applied pressure with $dT_C/dP = +3.5$ K kbar^{-1}. Given that the cell volume is almost identical in the orthorhombic and the rhombohedral structures (Asamitsu *et al.* 1995), the change in the pressure dependence of T_C is especially intriguing. To understand this we note that the Curie temperature, as well as the magnitude of the CMR effect in this class of materials, is sensitive to the Mn–O–Mn bond angle (Fontcuberta *et al.* 1996; Mitchell *et al.* 1996). When the crystal is compressed in the

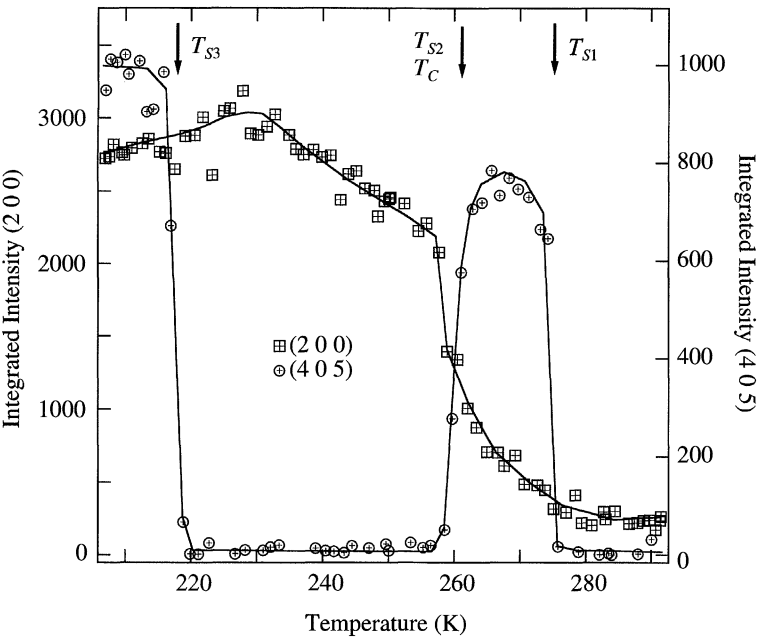

Figure 11. Temperature dependencies of the intensities of (4 0 5) and (2 0 0) reflections measured on heating at 2.6 kbar along the path AB on the phase diagram.

Pbnm phase, the Mn–O–Mn bonds are 'in-plane' and the pressure does not affect them much, changing instead the inter-plane distances. In the rhombohedral phase the 'easy' direction of compression is the three-fold axis which forms a non-zero angle to the Mn–O–Mn bonds. As a result, such bonds are affected more readily by applied pressure in the ($R\bar{3}c$) structure. In the pressure region above 3.0 kbar the temperature of the structural phase transition in the ferromagnetically ordered crystal decreases rapidly ($\mathrm{d}T_s/\mathrm{d}P = -10.0\,\mathrm{K\,kbar^{-1}}$).

The results of the isobaric temperature scans have allowed us to determine that the pressures 2.4 and 3.0 kbar are special for this phase diagram. Under a pressure of about 2.4 kbar, we observe a re-entrance of the rhombohedral ($R\bar{3}c$) phase, but this time within a ferromagnetically ordered state (Fr). As the temperature is decreased still further, the sample undergoes another phase transition to a ferromagnetic orthorhombic (Fo) phase. It is important to note that in the pressure region between 2.4 and 3.0 kbar the Po → Fo phase transition is still of a second order, i.e. there is no hysteresis. If the sample is cooled along the path BA on the *P–T* phase diagram without entering the Fr regime, then on heating, the reverse magnetic phase transition Fo → Po occurs at 261 K with no hysteresis. However, if the sample is cooled sufficiently to enter the Fr phase, then during a subsequent heating run, both the structural ($R\bar{3}c$) → *Pbnm* and the magnetic F → P phase transitions occur simultaneously as an Fr → Po transition. This behaviour is illustrated by the temperature dependence of the integrated intensities of (4 0 5) and (2 0 0) reflections measured during heating at a pressure of 2.6 kbar along the path AB on the *P–T* phase diagram (figure 11). As the temperature increases, the sample undergoes a series of structural phase transitions: *Pbnm* → ($R\bar{3}c$) at $T_{s3} = 238$ K,

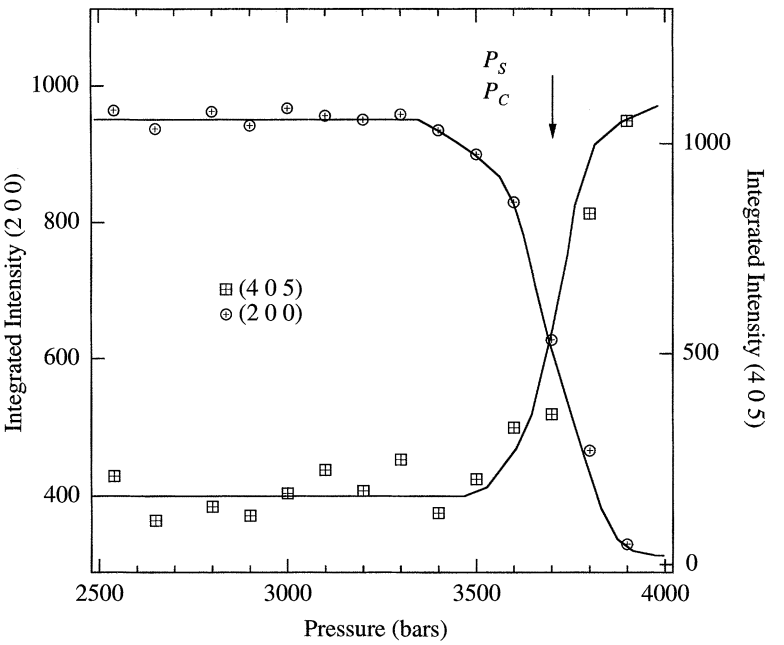

Figure 12. Pressure dependencies of the intensities of (4 0 5) and (2 0 0) reflections measured at $T = 270$ K with increasing pressure along the path FE on the P–T phase diagram.

$(R\bar{3}c) \rightarrow Pbnm$ at $T_{s2} = 264$ K and $Pbnm \rightarrow (R\bar{3}c)$ at $T_{s1} = 284$ K. The intensity of the magnetic (2 0 0) peak goes to zero at $T_C = 264$ K indicating that the magnetic phase transition occurs at the same temperature as the second structural transition. The hysteresis in temperature of the magnetic phase transition increases with pressure above 2.4 kbar, which means that in the hatched area the behaviour of the magnetic sublattice reflects the structural changes, switching the type of the magnetic phase transition from second to first order.

The phase transitions at T_{s1} and T_{s3} both lie on the same phase boundary separating the rhombohedral and the orthorhombic states, although we need to vary the pressure at a fixed temperature in order to complete this line and join these two points on the phase diagram. The changes in the intensities of the (4 0 5) and (2 0 0) reflections at $T = 270$ K during an increasing pressure scan along FE are presented in figure 12. The structural and magnetic phase transitions occur simultaneously at 3.0 kbar and 3.7 kbar for decreasing and increasing pressure respectively. Isothermal pressure scans below 261 K have shown that the Fr → Fo phase transition is induced by the release of pressure at pressures below 3.0 kbar. Due to the hysteretic character of the first-order structural phase transition and the fact that the magnetic transition is tied to it, in the hatched area of the crossing 'point' the sample can adopt either an Fr or a Po state depending on the pressure–temperature path by which it was brought into that area. It is also clear from the phase diagram that the boundary of the magnetic phase transition mirrors the hysteresis loop of the structural phase transition within the hatched area. This confirms our conclusion that, in this region of the phase diagram, it is the structural change which is driving the magnetic transition.

6. Conclusions

There is little doubt that the magnetic, structural and electronic properties of the compound $La_{1-x}Sr_xMnO_3$ are highly coupled, particularly in the region where the magnetic and structural phase transitions coincide. It is also likely that such arguments can be extended to include the fundamental excitations of the system, the phonons and magnons, producing a system with strong electron–magnon and electron–phonon coupling. Such an approach would suggest that some form of polaron would be the fundamental excitation of the system exhibiting both a magnetic and vibrational character. Extreme versions of such effects can be observed at the structural and magnetic phase transitions where there may be considerable changes in the lifetime, dispersion and stiffness of the fundamental excitations. These changes couple strongly with the ability of electrons to move through the system and therefore have a large influence on the transport properties.

A comparison of the effect of doping, magnetic field and pressure on the corresponding phase diagrams of $La_{1-x}Sr_xMnO_3$ ($x \sim 0.165$) reveals that increase in Sr (Mn^{4+}) content, magnetic field and/or pressure may be used to force a crossing of the Curie temperature with the temperature of the structural phase transition. Both critical temperatures are strongly dependent on the external variable at the crossing point and display unusual characteristics. In the case of an applied magnetic field, it appears that by producing an increased degree of ferromagnetic alignment it is possible to induce the structural rearrangement, while with applied pressure the magnetic transition is apparently controlled by the structural transformation. This is perhaps not too surprising since pressure and magnetic field are doing very different things to the system. In both cases a broad, hysteretic region forms at the crossover point, *ca.* 2 T for an applied field and *ca.* 3 kbar for applied pressure with $x = 0.165$, above and below these regions the hysteresis is much less. These, fairly initial, examinations of the structural and magnetic phase transitions still leave many questions unanswered but do suggest that extensions of such experiments will provide useful information on the microscopic properties of these systems and the fundamental interactions which control the structural, magnetic and electronic properties.

References

Asamitsu, A., Moritomo, Y., Tomioka, Y., Arima, T. & Tokura, Y. 1995 A structural phase-transition induced by an external magnetic-field. *Nature* **373**, 407.

Campbell, A. J., Balakrishnan, G., Lees, M. R., Paul, D. McK. & Mcintyre, G. J. 1997 Single-crystal neutron-diffraction study of a structural phase transition induced by a magnetic field in $La_{1-x}Sr_xMnO_3$. *Phys. Rev.* B **55**, R8622.

Fontcuberta, J., Martinez, B., Seffar, A., Pinol, S., Garcia-Munoz, J. L. & Obradors, X. 1996 Colossal magnetoresistance of ferromagnetic manganites—structural tuning and mechanisms. *Phys. Rev. Lett.* **76**, 1122–1125.

Jirak, Z., Krupicka, S., Simsa, Z., Dlouha, M. & Vratislav, S. 1985 Neutron diffraction study of $Pr_{1-x}Ca_xMnO_3$ perovskites. *J. Magn. Magn. Mat.* **53**, 153.

Kamenev, K., Balakrishnan, G., Lees, M. R., Paul, D. McK., Arnold, Z. & Mikulina, O. 1997 Influence of pressure on structural and magnetic phase transitions in $La_{0.835}Sr_{0.165}MnO_3$. *Phys. Rev.* B **56**, 2285–2287.

Kawano, H., Tokura, Y., Kajimoto, R., Kubota, M. & Yoshizawa, H. 1996 Ferromagnetism-induced re-entrant structural transition and phase diagram of the lightly doped insulator $La_{1-x}Sr_xMnO_3$ ($x = 0.17$). *Phys. Rev.* B **53**, R14709–14712.

Knizek, K., Jirak, Z., Pollert, E., Zounova, F. & Vratislav, S. 1992 Structure and magnetic properties of $Pr_{1-x}Ca_xMnO_3$ perovskites. *J. Solid State Chem.* **100**, 292.

Millis, A. J., Littlewood, P. B. & Shraiman, B. I. 1995 Double exchange alone does not explain the resistivity of $La_{1-x}Sr_xMnO_3$. *Phys. Rev. Lett.* **74**, 5144.

Mitchell, J. F., Argyriou, D. N., Potter, C. D., Hinks, D. G., Jorgensen, J. D. & Bader, S. D. 1996 Structural phase-diagram of $La_{1-x}Sr_xMnO_{3+d}$—relationship to magnetic and transport-properties. *Phys. Rev.* B **54**, 6172.

Radaelli, P. G., Marezio, M., Hwang, H. Y., Cheong, S. W. & Batlogg, B. 1996 Charge localization by static and dynamic distortions of the MnO_6 octahedra in perovskite manganites. *Phys. Rev.* B **54**, 8992.

Tokura, Y., Urushibara, A., Moritomo, Y., Arima, T., Asamitsu, A., Kido, G. & Furukawa, N. 1994 Giant magnetotransport phenomena in filling-controlled Kondo-lattice system — $La_{1-x}Sr_xMnO_3$. *J. Phys. Soc. Jpn* **63**, 3931–3935.

Wollan, E. O. & Koehler, W. C. 1955 Neutron diffraction study of the magnetic properties of the series of perovskite-type compounds $[(1-x)La,xCa]MnO_3$. *Phys. Rev.* **100**, 545.

Zener, C. 1951 Interaction between the d-shells in the transition metals. II. Ferromagnetic compounds of manganese with perovskite structure. *Phys. Rev.* **82**, 403.

Discussion

A. J. MILLIS (*The Johns Hopkins University, USA*). We return to figure 10, the phase diagram deduced from the neutron scattering. If I come down on the vertical line BA as the temperature decreases, I pass through a cross-hatched region which Dr Paul seems to imply is metastable and hysteretic, and then I cross the horizontal T_C line from a paramagnetic orthorhombic phase Po into a ferromagnetic orthorhombic phase Fo, a region that he believes is actually the stable equilibrium phase, and then I cross into Fr, the ferromagnetic rhombohedral phase. Why should I believe that? In other words, it is clear that at most one of those two phases is a thermodynamically stable phase and the other one I just get trapped into by accident; which one really has the lower free energy?

D. McK. PAUL. I'm saying that what you see depends on where you have been. If you come down the line BA and stop at a temperature just below the horizontal line, i.e. you remain in the Fo phase, then, on heating, the magnetic transition occurs at a temperature indicated by the horizontal line and the structural transition occurs at a somewhat higher temperature. However, if you cool down along BA all the way into the Fr phase, the magnetic and structural transitions, back to a paramagnetic orthorhombic phase, occur together at a temperature which is slightly higher than the magnetic transition temperature observed during cooling.

A. J. MILLIS. Where would I draw the line which actually indicates the place where the free energies cross as opposed to boundaries of some hysteresis region?

D. McK. PAUL. Depending on where I've been, where I've taken the sample to, I can produce several combinations of the phases in this particular region. But that tells you, I think, that the magnetism is trying to follow what you've done to the structure. I don't know what the true free energy is, if there is a true free energy, because it is history dependent.

P. BATTLE (*University of Oxford, UK*). This is being monitored by following the intensity of a couple of key reflections. Has Dr Paul actually refined the full crystal

structure, looked at a whole data set under different conditions? Is it possible he is getting different densities of twinning and domains, since there are various things that can be done to the crystals?

D. McK. Paul. There is certainly twinning, this is the reason why we haven't finished the complete refinement of the data set because there is twinning in these samples. If I stay in these clean regions I have no problem with that because I can go reproducibly backwards and forwards on some ferromagnetic scale and see the same intensities, the same ratios between reflections, so in that sense it looks to me as if the twinning distribution is not changing enormously. I can't be absolutely sure that it is not changing on a much smaller scale, but these are relatively big scales compared to that. So I think the answer is 'no', but we are trying to refine out some of these density distributions.

D. Khomskii (*University of Groningen, The Netherlands*). My question is connected with the one from Andy Millis. Would it be correct to think from Dr Paul's data that the rhombohedral phase has a stronger tendency to ferromagnetism than the orthorhombic one? It seems when that he goes back from rhombohedral up, his critical temperature for magnetic ordering is higher than from the orthorhombic phase.

D. McK. Paul. Well, yes possibly, except that all it's doing is sitting on the two hysteretic boundaries for the structural phase transition. Whether you think that implies that the rhombohedral has a higher tendency of being ferromagnetic than the orthorhombic or not, I'm not sure.

D. M. Edwards (*Imperial College, London, UK*). Dr Paul said that once he had changed the structure with the field, he couldn't go back to the previous structure. I seem to remember in the original paper of Asamitsu, they said that under certain conditions the structural transitions can be driven reversibly by a magnetic field. He didn't find that?

D. McK. Paul. Not in the range of temperatures examined by this experiment.

R. Stroud (*Naval Research Laboratory, Washington, USA*). What about the electronic degree of freedom which are also coupled to the structure?

D. McK. Paul. I'll tell you in a month or so, our problem is ridiculous but we cannot get our pressure cell into our magnet. A typical British problem—funding constraints.

T. Venkatesan (*University of Maryland, USA*). What is the composition that Dr Paul is using?

D. McK. Paul. The composition is 0.165 Sr doping. However, the properties of our crystal at 0.165 are identical to the Japanese crystals at 0.17. That we really don't understand, both of these are actually starting compositions and there may be very slight differences in oxygen content. These lines are incredibly steep so it wouldn't take very much, but what we call 0.165 Asamitsu would call 0.17.

J. R. Cooper (*University of Cambridge, UK*). In, for example, organic conductors it was a very common occurrence to have two competing phase transitions and two competing order parameters and people used to do very detailed theoretical analysis

and always when you had two competing order parameters you had regions with first order phase transitions, so you need a detailed theoretical analysis to tell you what is going on.

D. McK. Paul. Sure, but this is the first time we've seen this kind of thing in the manganite systems.

P. B. Littlewood (*University of Cambridge, UK*). We are used to the idea of competing order parameters. Here, I guess from the shape of that phase diagram, that the order parameters are attracting each other. Why else would you get that kink associated with the magnetism?

D. McK. Paul. You've got the order parameter that drives it from the orthorhombic and rhombohedral, then from paramagnetic to ferromagnetic at the same time. I agree, but I don't remember the sweeping re-entrant things as a function of pressure. It's definitely that they are competing and that it is an interacting system.

J. Pierre (*Laboratoire Louis Néel, Grenoble, France*). Has Dr Paul some idea of the directions for the spontaneous magnetisations in the orthorhombic and rhombohedral phases? Of course, there is only one Hamiltonian in the system and of course the magneto-hysteretic phenomena couple the magnetic ordering and the magnetostriction. How large are the magnetoelastic coefficients which couple magnetisation to the magnetostriction?

D. McK. Paul. Because of twinning a full analysis of the magnetic structure for these crystals has not yet been completed. Magnetoelastic measurements will be performed soon, when we can get the pressure cell into our magnet.

A. J. Millis. The fundamental question Dr Paul raised was, which was in charge? The structure or the magnetism? I wanted to offer a slightly different version of this question which was expressed to me very eloquently by Yoshi Tokura in Japan. He said, 'The question you're asking is which one is the chicken and which one is the egg?'

D. McK. Paul. Let me tell you another story about the charge ordering materials where you have are supposed to have a coincident electronic, magnetic, and structural phase transition. Every crystal we have looked at, we see several peaks in the specific heat. We've never found a crystal where we see one but you look at the bulk properties and everything seems to happen at the same point, but the specific heat seems to do all sorts of weird and wonderful things.